

pubs.acs.org/JPCL Letter

# Spectroscopically Quantifying the Influence of Salts on Nonionic Surfactant Chemical Potentials and Micelle Formation

Denilson Mendes de Oliveira and Dor Ben-Amotz\*



Cite This: J. Phys. Chem. Lett. 2021, 12, 355-360



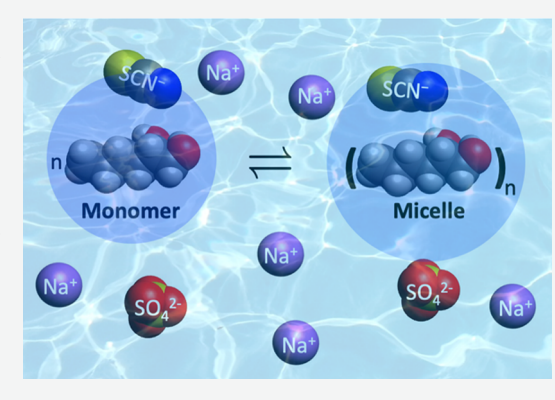
**ACCESS** 

Metrics & More



Supporting Information

**ABSTRACT:** The influence of two salts (NaSCN and Na<sub>2</sub>SO<sub>4</sub>) on the micellization of a nonionic surfactant (1,2-hexanediol) is quantified using Raman multivariate curve resolution spectroscopy, combined with a generalized theoretical analysis of the corresponding chemical potential changes. Although the SCN<sup>-</sup> and  $SO_4^{2-}$  anions are on opposite ends of the Hofmeister series, they are both found to lower the critical micelle concentration. Our combined spectroscopic and theoretical analysis traces these observations to the fact that in both salt solutions the ions have a greater affinity for (or are less strongly expelled from) the hydration shell of the micelle than the free surfactant monomer, as quantified using the corresponding chemical potentials and Wyman-Tanford coefficients. This probe-free experimental and theoretical analysis strategy may readily be extended to micelle formation processes involving other surfactants, salts, and cosolvents, as well as to other sorts of aggregation and binding processes.



Interactions between ions and aqueous molecular interfaces are important for numerous chemical and biological processes, including the solubility of nonelectrolytes, enzyme catalysis, 2,3 molecular self-assembly, 4-6 membrane permeability, 7,8 and cellular exocytosis. 9 Although the associated ion-specific (Hofmeister) effects 10-12 are in principle traceable to the influence of salts on molecular chemical potentials, open questions remain regarding the corresponding ion-molecule interactions. 12-15 Here we obtain such information by spectroscopically and theoretically analyzing the influence of two salts (NaSCN and Na<sub>2</sub>SO<sub>4</sub>) on the critical aggregation (micelle) concentration  $C_A$  of the nonionic surfactant 1,2hexanediol (12HD). We do so by combining Raman multivariate curve resolution (Raman-MCR) $^{16-23}$  measurements with a Wyman-Tanford $^{17,24-26}$  theoretical analysis. The results provide a means of spectroscopically quantifying  $C_A$  as well as the differential partitioning of the two salts into the hydration shells of the free surfactant monomer and micelle, and the associated chemical potential changes. Our results reveal that the stabilization of the micelle by both salts is linked to the greater ion concentration in the hydration shell of the micelle than the free 12HD monomer. Thus, the stabilization of the nonionic micelles by both these salts has much in common with the mechanisms by which polymer collapse and protein folding are enhanced by some salts and osmolytes. 27,28

Although some prior experimental and theoretical studies have described the influence of salts on the critical micelle concentration of 12HD and other nonionic surfactants, <sup>29–31</sup> none of these studies have characterized the effect of salts on the hydration shells of the monomeric and aggregated species

or quantitatively related the corresponding observations to the chemical potentials of both the free monomers and aggregates. The application of Raman-MCR to the elucidation of ionic micelle structures has previously been described, <sup>16</sup> but did not extend to nonionic surfactants or the influence of salts on micelle formation. Prior theoretical treatments of micelle salt effects have focused primarily on changes in the solubility of the free surfactant monomers, effectively treating the micelle as a reference state whose free energy is not significantly influenced by salts.<sup>29–31</sup> Moreover, these prior theoretical analyses have not attempted to relate the influence of salts on micelle formation to Wyman-Tanford theory. <sup>17,24–26</sup>

Raman-MCR is ideally suited to the quantitative analysis of surfactant solutions consisting of an equilibrium between free monomers and micelles, <sup>32,33</sup> since each of these species have distinct hydration-shell spectra (and surfactant spectral shifts). The self-modeling curve resolution (SMCR)<sup>23,34</sup> spectral decomposition strategy that we used begins with a first round of SMCR that removes bulk solvent contributions from each surfactant solution spectrum, to yield the corresponding surfactant-correlated (SC) spectrum. A second round of SMCR is then used to decompose the first round SC spectra

Received: November 9, 2020 Accepted: December 15, 2020 Published: December 23, 2020





into a linear combination of free monomer and micelle components and, thus, to quantify the micelle formation equilibrium and its salt dependence.

Wyman-Tanford theory  $^{17,24-26}$  can provide additional insight regarding the mechanism responsible for salt-induced changes in the critical micelle concentration. More specifically, this theory links the influence of salts on the micelle formation equilibrium  $(nM \rightleftharpoons M_n)$  to the partitioning of ions (and water) into the hydration shells of the micelle  $(M_n)$  and free monomer (M), as determined by the following partition coefficient.

$$\Gamma = \left\langle n_{\rm W} \left( \frac{n_{\rm S}}{n_{\rm W}} - \frac{N_{\rm S} - n_{\rm S}}{N_{\rm W} - n_{\rm W}} \right) \right\rangle \tag{1}$$

The variables  $N_i$  are the total numbers of molecules of type i in the system (where i=S for salt and i=W for water), whose values are determined by the total concentration of the solution. The variables  $n_i$  are the corresponding numbers of molecules in the surfactant hydration shell. Note that  $\Gamma$  will be equal to zero if the local salt-to-water ratio in the surfactant hydration shell,  $n_S/n_W$ , is equal to that far from the surfactant,  $(N_S-n_S)/(N_W-n_W)$ , and  $\Gamma$  will be positive if salt ions accumulate around the surfactant or negative if salt ions are expelled from the surfactant hydration shell.

Wyman-Tanford theory<sup>17</sup> yields the following expression for the influence of a salt of concentration  $C_S$  on the micelle formation equilibrium constant,  $K_n = [M_n]/[M]^n$ .

$$\frac{\mathrm{d} \ln K_{\mathrm{n}}}{\mathrm{d} \ln C_{\mathrm{S}}} = C_{\mathrm{S}} \left( \frac{\mathrm{d} \ln K_{\mathrm{n}}}{\mathrm{d} C_{\mathrm{S}}} \right) = \Delta \Gamma = \Gamma_{\mathrm{A}} - \Gamma_{\mathrm{F}}$$
(2)

Note that  $\Gamma_A$  pertains to a partitioning of salt (and water) to the hydration shell of the entire aggregate (micelle) containing n monomers, and  $\Gamma_F$  pertains to the hydration shells of a collection of n free monomers.

The partition coefficient difference  $\Delta\Gamma$  may be determined from the experimentally measured salt-induced change in the critical micelle concentration,  $\Delta C_{\rm A} = C_{\rm A}^{\rm S} - C_{\rm A}$ , where  $C_{\rm A}$  and  $C_{\rm A}^{\rm S}$  are the critical micelle concentrations in pure water and the salt solution, respectively. Moreover,  $\Delta\Gamma$  may be quantitatively linked to the derivative of the surfactant chemical potential with respect to salt concentration,  $k_{\rm i}$  (where i=1 for the free monomer and i=n for the micelle). Specifically, the relationship between  $\Delta\Gamma$ ,  $\Delta C_{\rm A}$ , and  $\Delta k=k_n-k_1$  is given by eq 3 (whose detailed derivation is provided in the Supporting Information, Section 3).

$$\Delta\Gamma = -n \left( \frac{\Delta C_{\rm A}}{C_{\rm A}} \right) = -n \left( \frac{\Delta k C_{\rm S}}{RT} \right) \tag{3}$$

Thus, a salt-induced decrease of the critical micelle concentration (i.e.,  $\Delta C_{\rm A} < 0$ , as observed experimentally) implies that  $\Gamma_{\rm A} > \Gamma_{\rm F}$  and  $k_1 > k_n$ , independent of the signs of  $\Gamma_{\rm A}$ ,  $\Gamma_{\rm F}$ ,  $k_1$ , and  $k_n$ . In other words, if salt ions are expelled from the hydration shells of both the free monomer and micelle, then eq 3 implies that salt invariably increases the surfactant chemical potential, but more so for the free monomer than the micelle. Conversely, if the salt concentration is enhanced in the hydration shells of both the free monomer and micelle, then eq 3 implies that salt decreases the surfactant chemical potential but less so for the micelle than the free monomer.

In this work, we used a probe-free Raman-MCR spectral decomposition strategy to determine both  $C_{\rm A}$  and  $\Delta C_{\rm A}$  for 12HD in pure water and aqueous salt solutions. We thus

demonstrate that Raman-MCR provides a direct means of experimentally determining both  $\Delta\Gamma$  and  $\Delta k$ , using the previously reported light-scattering measurement of the average micelle size of  $n\approx 20$  for 12HD in pure water. Moreover, the previously reported critical micelle concentration of 12HD in pure water  $0.53 \le C_A$ ,  $M \le 0.75$ , obtained using various methods,  $^{29,35}$  is consistent with the value of  $C_A = 0.60 \pm 0.02$  M that we obtained using Raman-MCR.

Figure 1A shows the measured Raman spectra of 12HD solutions at various concentrations. The Raman-MCR SC spectra shown in Figure 1B highlight differences between the solution and pure water spectra (obtained as described in the Supporting Information Section 1, with further details in refs 18, 21, and 22). These SC spectra reveal the following two changes with increasing 12HD concentration: (1) a decrease in the average CH frequency and (2) a decrease (depletion) in the area of the hydration shell OH stretch band.

The concentration dependence of the mean CH frequency shift, plotted in Figure 1C, has a sigmoidal shape characteristic of micelle formation, as the CH frequency of fully hydrated free monomers ( $\omega_{\rm CH} \approx 2907~{\rm cm}^{-1}$ ) decreases toward that in the substantially dehydrated micelles ( $\omega_{\rm CH} \approx 2902~{\rm cm}^{-1}$ ). The critical aggregation concentration  $C_{\rm A}$  roughly corresponds to the concentration at which the CH frequency becomes markedly nonlinearly concentration-dependent. A more precise identification of  $C_{\rm A}$  may be obtained from the results shown in Figure 1D, as further described below.

Since all the SC spectra in Figure 1B are normalized to the 12HD CH band area, the observed decrease (depletion) of the SC OH stretch band with increasing 12HD concentration is consistent with the aggregation-induced dehydration of 12HD, as previously observed in the aggregation of various monoalcohols in water,  $^{36-38}$  as well as in the formation of micelles from ionic surfactants.  $^{16}$  For dilute solutions ([12HD] $_{\rm T}$  < 0.5 M), there is only a small change in intensity of the hydration shell OH band, indicating that small aggregates do not significantly expel water molecules from the 12HD hydration shell, and thus the dehydration that is evident in Figure 1B is due primarily to micelle formation.

The family of OH stretch bands in Figure 1B arise from water molecules that are perturbed by 12HD, whose spectral shape differs from that of the OH stretch band of pure water, as indicated by the dashed blue curve in the inset panel in Figure 1B. Note that there are over 100 water OH groups in the first hydration shell of 12HD, so the two OH groups of 12HD do not significantly contribute to the SC spectra shown in Figure 1B (as further confirmed by the observation that the SC hydration shell OH band of dilute aqueous 12HD is essentially identical to that of 1-hexanol). 18

The SC spectra in Figure 1B may be quantitatively decomposed into a linear combination of free and aggregated component spectra, using a second-round SMCR analysis performed on all the SC spectra in Figure 1B (over a frequency range from 2375 to 3770 cm<sup>-1</sup>). More specifically, the low concentration SC spectrum is assigned to the free monomer, and the new second-round SMCR minimum area component, indicated by the dotted black curve in Figure 1B, is assigned to the 12HD molecules that are in a micelle. The robustness of this spectral decomposition is confirmed by noting that virtually identical aggregate spectra are obtained when using different high-concentration SC spectra as input for the second-round SMCR decomposition.

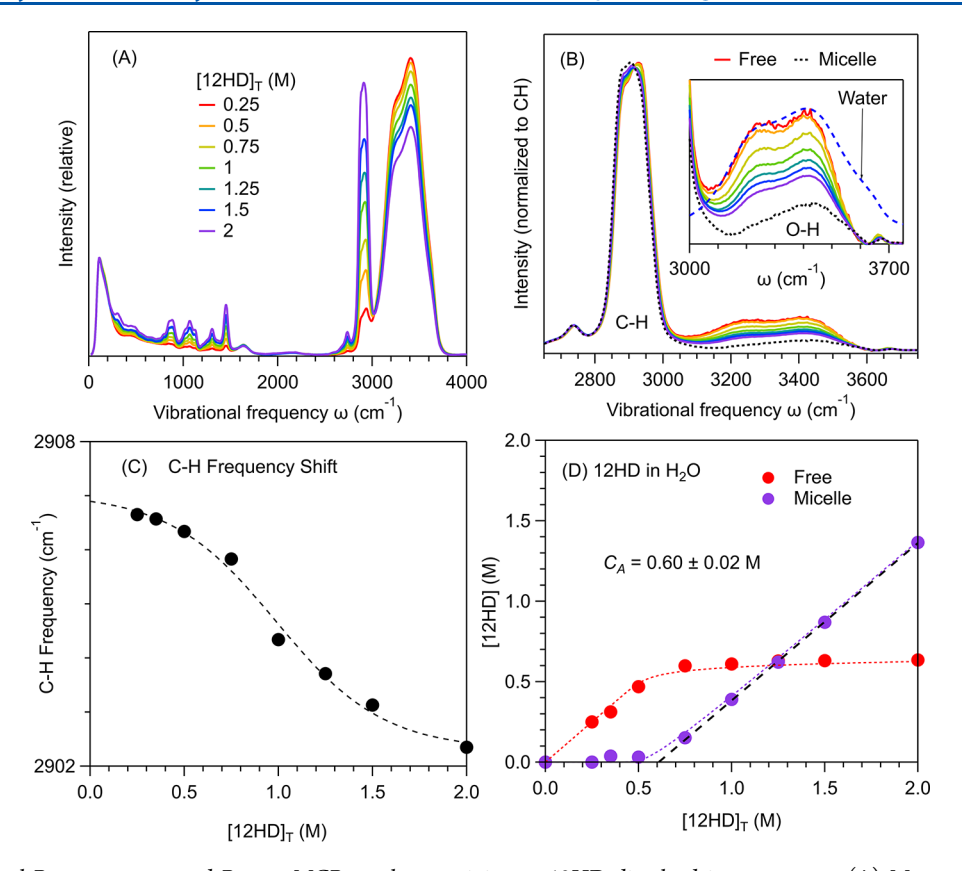


Figure 1. Experimental Raman spectra and Raman-MCR results pertaining to 12HD dissolved in pure water. (A) Measured Raman spectra of aqueous 12HD at 20 °C at various concentrations. (B) SC spectra of 12HD in the CH and OH stretch band region, normalized to the CH band area (after background subtraction). The inset figure in (B) shows an expanded view of the SC hydration shell OH stretch band region, including the OH bands of pure water (dashed blue curve) and the micelle hydration shell (dotted-black curve). (C) The mean CH frequency of 12HD is plotted as a function of the total surfactant concentration,  $[12HD]_T$ . (D) The concentrations of free and aggregated 12HD plotted as a function of  $[12HD]_T$ , obtained from a TLS fit of the SC spectra in (A) to a linear combination of the free (solid red curve) and aggregated (dotted-black curve) spectra. The dashed line in (D) is used to obtain  $C_A$  and the dotted curves are micelle formation equilibrium predictions (see text for details).

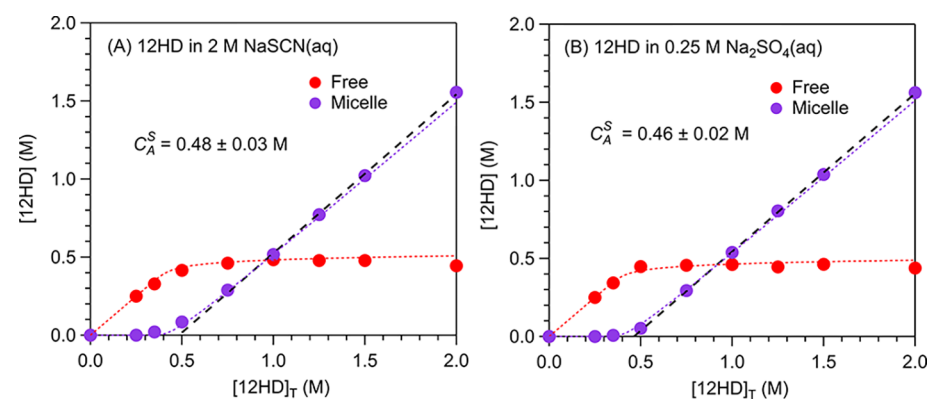


Figure 2. Raman-MCR results pertaining to 12HD dissolved in aqueous salt solutions containing either 2 M NaSCN or 0.25 M Na<sub>2</sub>SO<sub>4</sub>. (A) Free and aggregated 12HD concentrations in 2 M NaSCN. (B) Free and aggregated 12HD concentrations in 0.25 M Na<sub>2</sub>SO<sub>4</sub>. The dashed lines and dotted curves are obtained in the same way as those in Figure 1(D).

To determine the corresponding free and aggregated 12HD concentrations, we performed a total least-squares (TLS) regression fit of all the SC spectra to a linear combination of the free monomer SC spectrum (obtained at  $[12HD]_T = 0.25$  M) and micelle spectrum (dotted black curve in Figure 1B), as further described in the Supporting Information and refs 39 and 40. The results of this decomposition are indicated by the points in Figure 1D. As can be seen, virtually no aggregation

has taken place in dilute solutions of 12HD, but as the 12HD concentration is increased above ~0.5 M an abrupt change occurs, which is characteristic of the formation of higher-order aggregates when  $[12\text{HD}]_T > C_A$ . More specifically, we identify  $C_A$  as the x-axis intercept of a linear fit (dashed line) to the points corresponding to the concentration of aggregated 12HD molecules, performed over a concentration range of  $0.7 \le [12\text{HD}]_T$ ,  $M \le 2$ , to obtain  $C_A = 0.60 \pm 0.02$  M for 12HD in

pure water, in good agreement with previous estimates. Further validation of our assignments of the component spectra is provided by the good agreement between the experimental points in Figure 1D and the dotted curves obtained assuming a micelle formation equilibrium with n = 20 and  $C_{\rm A} = 0.60$  M (as explained in the Supporting Information, Section 3).

To quantify the influence of salts on the 12HD micelle formation, we performed Raman-MCR measurements on ternary mixtures containing 12HD, water, and either 2 M NaSCN or 0.25 M Na<sub>2</sub>SO<sub>4</sub> (as at these concentrations the two salts produced a similar influence on the 12HD micelle formation). The salt concentration was held constant, while the 12HD concentration was varied, such that the aqueous salt solution was treated as the solvent and 12HD as the solute in the subsequent SMCR decompositions (which were otherwise performed as described above).

Figure 2 shows the concentrations of 12HD in the free monomer and micelle in (A) 2 M NaSCN and (B) 0.25 M  $Na_2SO_4$ . These concentrations were obtained in the same way as those in Figure 1D, using the free monomer and micelle component spectra pertaining to the corresponding salt solution (shown in the Supporting Information Figure S1). The resulting critical aggregation concentrations  $C_A^S$  and dotted curves in Figure 2 were obtained in the same way as those in Figure 1D. Comparison of these  $C_A^S$  values with the  $C_A$  in pure water (see Figure 1D) reveals that the critical micelle concentrations in the salt solutions are both lower than that in pure water, thus indicating that both salts stabilize the micelle with respect to the free monomer.

More quantitative information regarding the influence of the salts on 12HD micelle formation may be obtained by using the measured  $\Delta C_A = C_A^S - C_A$  to determine both  $\Delta k$  and  $\Delta \Gamma$ (using eq 3) and, thus, quantify the differential affinities of the ions for the free and aggregated 12HD molecules, as well as the corresponding chemical potential changes. The salt-induced decrease in the critical micelle concentration implies that  $\Delta C_A/C_A = -0.20 \pm 0.01$  in 2 M NaSCN and that  $\Delta C_A/C_A =$  $-0.23 \pm 0.01$  in 0.25 M Na<sub>2</sub>SO<sub>4</sub>. Given that there are approximately n = 20 surfactant molecules in each micelle, <sup>35</sup> eq 3 implies that  $\Delta\Gamma \approx 4.0$  in aqueous NaSCN and  $\Delta\Gamma \approx 4.6$  in aqueous Na<sub>2</sub>SO<sub>4</sub>. Moreover, eq 3 further indicates that  $\Delta k \approx$ -0.24 and -2.2 kJ/mol M<sup>-1</sup> in aqueous NaSCN and Na<sub>2</sub>SO<sub>4</sub>, respectively, in keeping with the fact that a nearly 10 times higher NaSCN concentration is required to produce a similar decrease in  $C_A$ .

Although the values of  $\Delta\Gamma$  and  $\Delta k$  are directly measurable, as described above, determining the signs and magnitudes of  $\Gamma_A$ ,  $\Gamma_E$ ,  $k_n$ , and  $k_1$  requires additional information. Raman-MCR provides some such information, as it indicates that SCNanions penetrate significantly into the hydration shell of 12HD, while  $SO_4^{\ 2-}$  anions do not. The interaction between 12HD and SCN- is evidenced not only by the NaSCN-induced changes in the hydration shell spectra of both the free 12HD monomer and micelle (see Supporting Information Figure S1) but also by changes in the C≡N band of SCN<sup>-</sup> induced by its interactions with both the free monomer and micelle (see Supporting Information Figures S2 and S3). No such interactions are seen in 0.25 M Na<sub>2</sub>SO<sub>4</sub> (Figures S1 and S4). These observations imply that the values of both  $k_1$  and  $k_n$  are positive for 12HD in 0.25 M Na<sub>2</sub>SO<sub>4</sub>, while in 2 M NaSCN both  $k_1$  and  $k_n$  have smaller magnitudes and may, perhaps, be negative.

Additional constraints on the range of physically reasonable values of  $k_1$  and  $k_n$  may be obtained by considering the consequences of assuming either that the salt has no effect on the chemical potential of the micelle or that the local salt concentration in the hydration shell of 12HD is the same for the free monomer and micelle (as further explained in the Supporting Information, Section 4). Such considerations lead to the conclusion that  $2.2 \le k_1 \le 5.9$  (kJ/mol M<sup>-1</sup>) in 0.25 M Na<sub>2</sub>SO<sub>4</sub>, while in 2 M NaSCN  $k_1$  is ~10 times smaller and  $k_n$  is smaller still and may, perhaps, be negative. The corresponding range of the Wyman-Tanford partition coefficient estimates are  $-12 < \Gamma_F \le -5$  in 0.25 M Na<sub>2</sub>SO<sub>4</sub> and  $-6 \le \Gamma_F \le -4$  in 2 M NaSCN (as further explained in the Supporting Information, Section 4), and thus  $\Gamma_A$  in aqueous NaSCN must be near zero and may, perhaps, be positive.

In summary, we have used a new probe-free Raman-MCRbased spectral decomposition strategy to determine the critical micelle concentration of a nonionic surfactant 12HD in pure water and aqueous NaSCN and Na2SO4. The resulting surfactant-correlated spectra reveal that SCN- anions penetrate significantly into the hydration shell of 12HD, while SO<sub>4</sub><sup>2-</sup> anions do not. A Wyman-Tanford analysis strategy is used to quantify the partitioning of these ions into the surfactant hydration shell, and the resulting salt-induced chemical potential changes. Our results explain how it is that these ions on opposite ends of the Hofmeister series produce a similar reduction in the critical micelle concentration, as in both cases the ion-induced stabilization of the micelles is due to the greater ion affinity for (or weaker expulsion from) the hydration shell of the micelle than the free surfactant monomer. The Raman-MCR and Wyman-Tanford strategy is quite general and thus could be extended to other micelle formation, binding, and folding processes.

### ASSOCIATED CONTENT

## **Supporting Information**

The Supporting Information is available free of charge on the ACS Publications Web site: The Supporting Information is available free of charge at https://pubs.acs.org/doi/10.1021/acs.jpclett.0c03349.

Experimental methods; additional experimental results; derivation of micellization and Wyman-Tanford expressions; Wyman-Tanford partition coefficient bounds (PDF)

## AUTHOR INFORMATION

#### **Corresponding Author**

Dor Ben-Amotz — Department of Chemistry, Purdue University, West Lafayette, Indiana 47907, United States; orcid.org/0000-0003-4683-5401; Email: bendor@purdue.edu

#### Author

Denilson Mendes de Oliveira — Department of Chemistry, Purdue University, West Lafayette, Indiana 47907, United States; ⊚ orcid.org/0000-0002-2579-8405

Complete contact information is available at: https://pubs.acs.org/10.1021/acs.jpclett.0c03349

### Notes

The authors declare no competing financial interest.

#### ACKNOWLEDGMENTS

This work was supported by the National Science Foundation (CHE-1763581). We also thank J. R. Dohrman for performing preliminary measurements related to this work (as part of his undergraduate research project) and A. S. Urbina for performing the molecular dynamics simulations used to obtain an estimate of the number of water molecules in the hydration shell of a nonaggregated 1,2-hexanediol molecule (as described in the Supporting Information).

### REFERENCES

- (1) Pegram, L. M.; Record, M. T. Thermodynamic origin of Hofmeister ion effects. J. Phys. Chem. B 2008, 112, 9428–9436.
- (2) Salis, A.; Bilaničová, D.; Ninham, B. W.; Monduzzi, M. Hofmeister effects in enzymatic activity: Weak and strong electrolyte influences on the activity of Candida rugosa lipase. *J. Phys. Chem. B* **2007**, *111*, 1149–1156.
- (3) Bilaničová, D.; Salis, A.; Ninham, B. W.; Monduzzi, M. Specific anion effects on enzymatic activity in nonaqueous media. *J. Phys. Chem. B* **2008**, *112*, 12066–12072.
- (4) Abezgauz, L.; Kuperkar, K.; Hassan, P. A.; Ramon, O.; Bahadur, P.; Danino, D. Effect of Hofmeister anions on micellization and micellar growth of the surfactant cetylpyridinium chloride. *J. Colloid Interface Sci.* **2010**, 342, 83–92.
- (5) Lin, S.-T.; Lin, C.-S.; Chang, Y.-Y.; Whitten, A. E.; Sokolova, A.; Wu, C.-M.; Ivanov, V. A.; Khokhlov, A. R.; Tung, S.-H. Effects of alkali cations and halide anions on the self-assembly of phosphatidylcholine in oils. *Langmuir* **2016**, 32, 12166–12174.
- (6) Mortara, L.; Lima, F. d. S.; Cuccovia, I. M.; Nazet, A.; Horinek, D.; Buchner, R.; Chaimovich, H. Specific ion effects on zwitterionic micelles are independent of interfacial hydration changes. *Langmuir* **2018**, *34*, 11049–11057.
- (7) Visser, H. C.; Rudkevich, D. M.; Verboom, W.; de Jong, F.; Reinhoudt, D. N. Anion carrier mediated membrane transport of phosphate: Selectivity of H<sub>2</sub>PO<sub>4</sub><sup>-</sup> over Cl<sup>-</sup>. *J. Am. Chem. Soc.* **1994**, *116*, 11554–11555.
- (8) Petrache, H. I.; Zemb, T.; Belloni, L.; Parsegian, V. A. Salt screening and specific ion adsorption determine neutral-lipid membrane interactions. *Proc. Natl. Acad. Sci. U. S. A.* **2006**, *103*, 7982.
- (9) He, X.; Ewing, A. G. Counteranions in the stimulation solution alter the dynamics of exocytosis consistent with the Hofmeister series. *J. Am. Chem. Soc.* **2020**, *142*, 12591–12595.
- (10) Hofmeister, F. Zur Lehre von der Wirkung der Salze. *Naunyn-Schmiedeberg's Arch. Pharmacol.* **1888**, 25, 1–30.
- (11) Kunz, W.; Henle, J.; Ninham, B. W. 'Zur Lehre von der Wirkung der Salze' (About the science of the effect of salts): Franz Hofmeister's historical papers. *Curr. Opin. Colloid Interface Sci.* **2004**, 9. 19–37.
- (12) Jungwirth, P.; Cremer, P. S. Beyond Hofmeister. *Nat. Chem.* **2014**, *6*, 261–263.
- (13) Gurau, M. C.; Lim, S.-M.; Castellana, E. T.; Albertorio, F.; Kataoka, S.; Cremer, P. S. On the mechanism of the Hofmeister effect. *J. Am. Chem. Soc.* **2004**, *126*, 10522–10523.
- (14) Zhang, Y.; Cremer, P. S. The inverse and direct Hofmeister series for lysozyme. *Proc. Natl. Acad. Sci. U. S. A.* **2009**, *106*, 15249–15253.
- (15) Zhang, Y.; Furyk, S.; Bergbreiter, D. E.; Cremer, P. S. Specific ion effects on the water solubility of macromolecules: PNIPAM and the Hofmeister series. *J. Am. Chem. Soc.* **2005**, *127*, 14505–14510.
- (16) Long, J. A.; Rankin, B. M.; Ben-Amotz, D. Micelle Structure and Hydrophobic Hydration. *J. Am. Chem. Soc.* **2015**, *137*, 10809–10815.
- (17) Mochizuki, K.; Pattenaude, S. R.; Ben-Amotz, D. Influence of cononsolvency on the aggregation of tertiary butyl alcohol in methanol-water mixtures. *J. Am. Chem. Soc.* **2016**, *138*, 9045–9048.

- (18) Davis, J. G.; Gierszal, K. P.; Wang, P.; Ben-Amotz, D. Water structural transformation at molecular hydrophobic interfaces. *Nature* **2012**, *491*, 582–585.
- (19) Wu, X. E.; Lu, W. J.; Streacker, L. M.; Ashbaugh, H. S.; Ben-Amotz, D. Temperature-dependent hydrophobic crossover length scale and water tetrahedral order. *J. Phys. Chem. Lett.* **2018**, *9*, 1012–1017.
- (20) Wu, X. E.; Lu, W. J.; Streacker, L. M.; Ashbaugh, H. S.; Ben-Amotz, D. Methane hydration-shell Structure and fragility. *Angew. Chem., Int. Ed.* **2018**, *57*, 15133–15137.
- (21) Rankin, B. M.; Hands, M. D.; Wilcox, D. S.; Fega, K. R.; Slipchenko, L. V.; Ben-Amotz, D. Interactions between halide anions and a molecular hydrophobic interface. *Faraday Discuss.* **2013**, *160*, 255–270.
- (22) Gierszal, K. P.; Davis, J. G.; Hands, M. D.; Wilcox, D. S.; Slipchenko, L. V.; Ben-Amotz, D. π-Hydrogen bonding in liquid water. *I. Phys. Chem. Lett.* **2011**, 2, 2930–2933.
- (23) Perera, P.; Wyche, M.; Loethen, Y.; Ben-Amotz, D. Solute-induced perturbations of solvent-shell molecules observed using multivariate Raman curve resolution. *J. Am. Chem. Soc.* **2008**, *130*, 4576–4577.
- (24) Mondal, J.; Halverson, D.; Li, I. T.; Stirnemann, G.; Walker, G. C.; Berne, B. J. How osmolytes influence hydrophobic polymer conformations: A unified view from experiment and theory. *Proc. Natl. Acad. Sci. U. S. A.* **2015**, *112*, 9270–9275.
- (25) Wyman, J., Jr. Advances in protein chemistry; Elsevier, 1964; Vol. 19, pp 223–286.
- (26) Tanford, C. Extension of the theory of linked functions to incorporate the effects of protein hydration. *J. Mol. Biol.* **1969**, 39, 539–544.
- (27) Bruce, E. E.; Okur, H. I.; Stegmaier, S.; Drexler, C. I.; Rogers, B. A.; van der Vegt, N. F. A.; Roke, S.; Cremer, P. S. Molecular mechanism for the interactions of Hofmeister cations with macromolecules in aqueous solution. *J. Am. Chem. Soc.* **2020**, *142*, 19094.
- (28) Ganguly, P.; Polák, J.; van der Vegt, N. F. A.; Heyda, J.; Shea, J.-E. Protein stability in TMAO and mixed urea-TMAO solutions. *J. Phys. Chem. B* **2020**, *124*, 6181–6197.
- (29) Francisco, O. A.; Glor, H. M.; Khajehpour, M. Salt effects on hydrophobic solvation: Is the observed salt specificity the result of excluded volume effects or water mediated ion-hydrophobe association? *ChemPhysChem* **2020**, 21, 484–493.
- (30) Ray, A.; Nemethy, G. Effects of ionic protein denaturants on micelle formation by nonionic detergents. *J. Am. Chem. Soc.* **1971**, 93, 6787–6793.
- (31) Koroleva, S. V.; Korchak, P.; Victorov, A. I. Molecular thermodynamic modeling of the specific effect of salt on the aggregation of nonionic surfactants. *J. Chem. Eng. Data* **2020**, *65*, 987–992
- (32) Ben-Amotz, D. Understanding Physical Chemistry; John Wiley and Sons: New York. 2014.
- (33) Israelachvili, J. N. *Intermolecular and Surface Forces*, 2nd ed.; Academic Press: San Diego, CA, 1991.
- (34) Lawton, W. H.; Sylvestre, E. A. Self modeling curve resolution. *Technometrics* **1971**, *13*, 617–633.
- (35) Hajji, S. M.; Errahmani, M. B.; Coudert, R.; Durand, R. R.; Cao, A.; Taillandier, E. A comparative study of 1,2-hexanediol and 1,2,3-octanetriol in aqueous solutions by different physical techniques. *J. Phys. Chem.* **1989**, 93, 4819–4824.
- (36) Wilcox, D. S.; Rankin, B. M.; Ben-Amotz, D. Distinguishing aggregation from random mixing in aqueous t-butyl alcohol solutions. *Faraday Discuss.* **2014**, *167*, 177–190.
- (37) Rankin, B. M.; Ben-Amotz, D.; van der Post, S. T.; Bakker, H. J. Contacts between alcohols in water are random rather than hydrophobic. *J. Phys. Chem. Lett.* **2015**, *6*, 688–692.
- (38) Bredt, A. J.; Ben-Amotz, D. Influence of crowding on hydrophobic hydration-shell structure. *Phys. Chem. Chem. Phys.* **2020**, 22, 11724–11730.

- (39) Mendes de Oliveira, D.; Ben-Amotz, D. Cavity hydration and competitive binding in methylated  $\beta$ -cyclodextrin. *J. Phys. Chem. Lett.* **2019**, *10*, 2802–2805.
- (40) Mendes de Oliveira, D.; Zukowski, S. R.; Palivec, V.; Hénin, J.; Martinez-Seara, H.; Ben-Amotz, D.; Jungwirth, P.; Duboué-Dijon, E. Binding of divalent cations to acetate: Molecular simulations guided by Raman spectroscopy. *Phys. Chem. Chem. Phys.* **2020**, 22, 24014—24027.